

## Atmospheric anomalies observed during earthquake occurrences

H. Fujiwara,<sup>1</sup> M. Kamogawa,<sup>2</sup> M. Ikeda,<sup>3</sup> J. Y. Liu,<sup>4</sup> H. Sakata,<sup>2</sup> Y. I. Chen,<sup>5</sup> H. Ofurton,<sup>6</sup> S. Muramatsu,<sup>7</sup> Y. J. Chuo,<sup>8</sup> and Y. H. Ohtsuki<sup>1</sup>

Received 2 March 2004; revised 26 July 2004; accepted 4 August 2004; published 11 September 2004.

[1] Appearance of anomalies in the atmosphere before earthquakes (EQs) has been verified, through observation of anomalous transmission of VHF electromagnetic (EM) waves beyond line-of-sight. Anomalous increase of the received intensity for a few minutes - several hours on a day was identified by the previous 15-day running median and its inter-quartile range. The cross-correlation between the EQ occurrences and the anomalies shows that the appearance of anomalies was significantly enhanced within 5 days before  $M \geq 4.8$  EQs. The one-day average number of the anomaly appearance within 5 days was found 2.4 times larger than that of other days. Through the polarization measurement of the received EM waves, the anomalies were found to occur in the atmosphere. **INDEX TERMS:** 6904 Radio Science: Atmospheric propagation; 6964 Radio Science: Radio wave propagation; 7223 Seismology: Seismic hazard assessment and prediction. **Citation:** Fujiwara, H., M. Kamogawa, M. Ikeda, J. Y. Liu, H. Sakata, Y. I. Chen, H. Ofurton, S. Muramatsu, Y. J. Chuo, and Y. H. Ohtsuki (2004), Atmospheric anomalies observed during earthquake occurrences, *Geophys. Res. Lett.*, 31, L17110, doi:10.1029/2004GL019865.

### 1. Introduction

[2] Studies of seismo-electromagnetics (seismo-EM) have been developed for a few decades. In particular, the ionospheric anomalies associated with EQs have been investigated since the 1980s [e.g., *Molchanov and Hayakawa*, 1998; *Liu et al.*, 2000].

[3] The VHF electromagnetic waves cannot usually propagate long distance [Davies, 1990] because they penetrate through the ionosphere. They can reach far away receivers beyond the line-of-sight only when reflection and scattering due to ionospheric or atmospheric disturbances take place. Such disturbances include Sporadic E-layer (Es-layer) and meteor generated plasma tubes. Therefore, VHF EM waves can be used for monitoring them. It is possible to investigate the transmission path of the waves through measuring their polarization as applied for VHF radars.

[4] *Kushida and Kushida* [2002] reported the empirical relationship between EQ occurrences and the anomalous receptions of FM radio waves. Since this kind of observation system was widely used for meteor observation, they proposed that the observed preseismic FM radio waves were also reflected at disturbed ionosphere. Related studies have been also made [e.g., *Sakai et al.*, 2001].

[5] Although there are a number of reports on the existence of the preseismic anomalies, it is still difficult to verify them owing to the lack of reproducibility and definitive criteria. Since the seismo-EM methods cannot directly monitor what is happening electromagnetically around hypocenter before EQs, it is difficult to prove that observed preseismic anomalies are truly precursory. Therefore, the inductive reasoning as used in the epidemiology would be required.

[6] This paper reports two aspects. One is the result of our VHF EM wave measurements to decipher whether the source of the anomalies are in ionosphere or atmosphere and the other is our effort to establish the precursory nature of the observed phenomena through inductive reasoning.

### 2. Observation and Analysis

[7] A receiver was located in Hidaka (E139°18'4.67", N35°52'15.76", altitude: 150 m), Japan as shown in Figure 1. The FM radio station, emitting horizontally polarized 77.1 MHz (5 kW), is located in Sendai (E140°52'41.9", N38°15'43.1", altitude: 193 m). The distance between the receiver and the transmitter is approximately 294 km that is over-the-horizon length. For reference, we concurrently monitored the Oita and Kyoto stations. The target area, shown by the gray rectangle in Figure 1, is seismically highly active.

[8] For receiving the VHF waves, two 5-element Yagi antennas were used for each station, and receivers had IF filters with 100 kHz bandwidth at -3 dBm. Elements of the antennas were horizontally and vertically installed in the direction of each station. The elevation angle of all antennas was 0 degree. There is a nearby FM radio station of the same 77.1 MHz. However, while the neighboring radio station dose not usually broadcast during the midnight, our target radio station broadcasts almost 24 hours. Therefore, we used only midnight data. The sampling rate was 1 Hz.

[9] In order to compare the EQ occurrences and the observed anomalies, definitive criteria for extracting the anomaly should be specified. *Molchanov and Hayakawa* [1998] defined the anomaly as the value in excess of 2 times of monthly standard deviation. In order to avoid the influence of the main shock, and the aftershocks on monthly standard deviation, *Liu et al.* [2000] defined the anomaly as the value in excess of the upper or lower bounds of the previous 15-day running inter-quartile ranges. We adopt the

<sup>1</sup>Department of Physics, Waseda University, Tokyo, Japan.

<sup>2</sup>Department of Physics, Tokyo Gakugei University, Tokyo, Japan.

<sup>3</sup>Shintech Company Limited, Tokyo, Japan.

<sup>4</sup>Institute of Space Science, National Central University, Chung-Li, Taiwan.

<sup>5</sup>Institute of Statistics, National Central University, Chung-Li, Taiwan.

<sup>6</sup>Tokyo Metropolitan College of Aeronautical Engineering, Tokyo, Japan.

<sup>7</sup>San-Eye Company Limited, Ehime, Japan.

<sup>8</sup>Department of Information Management, Ling-Tung College, Tai-Chung, Taiwan.

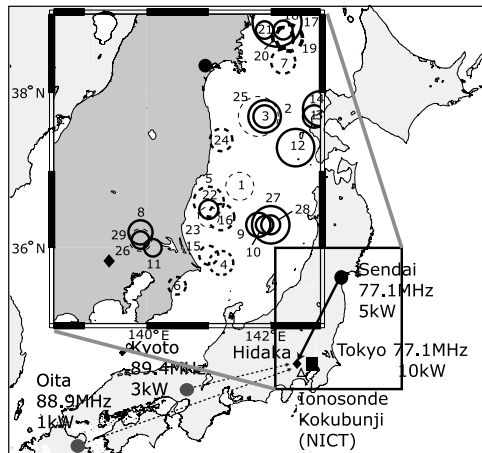


**Figure 1.** Solid circle, gray circles, and solid diamond represent the location of the transmitter, the reference transmitters, and the receiver, respectively. Open triangle represents the ionosonde location operated by National Institute of Information and Communications Technology (NICT), Japan. Gray rectangle represents the target area. In the upper left, the EQs inside the gray rectangle are shown. Open circles, open dotted circles, and open gray-dotted circles represent the EQs with preseismic anomalies, without anomalies, and no data, respectively.

same definition. The threshold of magnitude of our target EQs was set to 4.8. The length of 15 days was suitable in our case because the average recurrence interval of our target EQs ( $M \geq 4.8$ ) was more than 15 days. The restricted length of usable time each day (a few midnight hours) required two methods for analysis. One was to describe the

variations longer than a few hours (long period) and the other was to describe shorter variations in the range from a few tens of minutes to a few hours (short period). In order to obtain the one-day data  $X(T)$ , the long period variations (LPV) and short period variations (SPV) are expressed by

$$X_{LPV}(T) = \text{Median}\{x(0), x(1), \dots, x(t), \dots\} \quad (1)$$

$$X_{SPV}(T) = \text{Max}\{\tilde{x}(0), \tilde{x}(1), \dots, \tilde{x}(t), \dots\} \\ - \text{Median}\{\tilde{x}(0), \tilde{x}(1), \dots, \tilde{x}(t), \dots\} \quad (2)$$

where  $T$  is the date,  $x$  is the observed amplitude,  $t$  is time, and  $\{\tilde{x}(0), \tilde{x}(1), \dots, \tilde{x}(t), \dots\}$  is data after wavelet high frequency noise-reduction. Both  $X_{LPV}$  and  $X_{SPV}$  are less influenced by noises.

[10] Since the distribution of the time series  $X(T)$  had a long tail, the same method as proposed by Liu *et al.* [2000] was applied. The threshold value of anomaly was as follows. The one-day data  $X(T)$  is compared with the upper bound  $X^{UB}(T)$  (threshold value) defined by

$$X^{UB}(T) = X^{\text{Median}}(T) + K \cdot X^{\text{IQR}}(T) \quad (3)$$

where

$$X^{\text{Median}} = \text{Median}\{X(T-15), \dots, X(T-1)\},$$

$$X^{\text{IQR}} = \text{Third Quartile}\{X(T-15), \dots, X(T-1)\} \\ - \text{First Quartile}\{X(T-15), \dots, X(T-1)\},$$

and  $K$  is the coefficient related to the threshold value. Note that only  $X(T)$  larger than  $X^{UB}(T)$  would be meaningful for

**Table 1.** List of  $M \geq 4.8$  EQs and the Preseismic Anomalies<sup>a</sup>

No.	Day	Time	Lat.	Lon.	Dept.	M	SPV	LPV
1	2001/9/4	23:54	N36.8	E141.5	40 km	5.4	no upper bound	no upper bound
2	2001/10/2	17:20	N37.7	E141.9	40 km	5.6	2001/9/27	2001/9/28
3	2002/1/29	8:45	N37.7	E141.9	40 km	5.1		2002/1/27, 1/29
4	2002/2/11	10:10	N35.8	E141.2	50 km	5.2		
5	2002/2/12	22:44	N36.6	E141.0	40 km	5.5		
6	2002/5/4	20:35	N35.5	E140.5	40 km	4.8		
7	2002/5/6	17:12	N38.4	E142.2	40 km	5.2		
8	2002/6/14	11:42	N36.2	E139.9	50 km	5.2		2002/6/9, 6/10, 6/11
9	2002/6/19	18:16	N36.3	E141.8	20 km	5.2	2002/6/16, 6/19	
10	2002/7/9	22:53	N36.3	E141.9	60 km	4.8	2002/7/4	
11	2002/7/13	21:45	N36.0	E140.1	70 km	4.8	2002/7/11, 7/13	
12	2002/7/24	5:05	N37.3	E142.4	20 km	5.8	2002/7/20	
13	2002/10/11	10:04	N37.7	E142.7	10 km	5.1	2002/10/7	
14	2002/10/12	19:59	N37.8	E142.8	10 km	5.7	2002/10/7	
15	2002/10/16	13:04	N35.9	E141.0	40 km	4.9		
16	2002/10/21	1:06	N36.4	E141.2	40 km	5.3		
17	2002/11/3	12:37	N38.9	E142.1	50 km	6.2	2002/10/29, 10/31, 11/2	
18	2002/11/4	4:14	N38.8	E142.2	50 km	4.9	after shock	after shock
19	2002/12/5	0:50	N38.7	E142.3	40 km	5.3		
20	2002/12/5	0:53	N38.7	E142.2	40 km	5.0	after shock	after shock
21	2003/1/5	18:51	N38.8	E141.9	100 km	4.8	2003/1/3, 1/4	
22	2003/1/9	13:14	N36.5	E141.0	30 km	4.9	2003/1/4	
23	2003/1/21	13:19	N36.4	E141.0	40 km	5.0	no upper bound	no upper bound
24	2003/2/16	12:03	N37.4	E141.2	70 km	5.1		
25	2003/3/3	7:47	N37.7	E141.8	40 km	5.9	no data	no data
26	2003/3/13	12:13	N36.1	E139.9	50 km	5.1	no upper bound	no upper bound
27	2003/4/8	3:28	N36.3	E142.0	20 km	5.8	2003/4/6	
28	2003/4/8	4:16	N36.3	E142.0	70 km	4.9	2003/4/6	
29	2003/4/8	4:17	N36.1	E139.9	50 km	4.8	2003/4/6	

<sup>a</sup>EQ catalog: National Research Institute for Earth Science and Disaster Prevention (NIED), Japan.

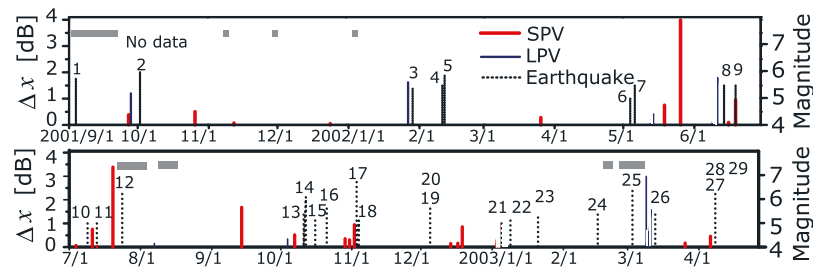


**Figure 2.** Time-series of  $\Delta X$  in LPV (blue) and SPV (red). EQ occurrences are depicted by the dotted line. ( $K = 2.4$ ).

anomaly detection. The value  $\Delta X(T)$  that represents the difference between  $X(T)$  and  $X^{UB}(T)$  was additionally introduced by

$$\Delta X(T) \equiv \begin{cases} 0 & (X(T) \leq X^{UB}(T)) \\ X(T) - X^{UB}(T) & (X(T) > X^{UB}(T)) \end{cases} \quad (4)$$

Positive  $\Delta X(T)$  means the anomaly. Note that the non-local phenomena were excluded in the time-series  $\Delta X(T)$  using the reference observation.

### 3. Results and Discussion

[11] By the aforementioned processes, the time-series of  $\Delta X(T)$  during the occurrences of the  $M \geq 4.8$  EQs listed in Table 1 were obtained as shown in Figure 2, in which  $K = 2.4$  was used. The observation period was from September, 2001 to April, 2002 (one year and 8 months including no data periods). In the next stage, the number of the anomalies within 15 days before and after each EQ was counted as shown in Figure 3a. As shown in Figure 3b, the z-test at level 0.01 showed that, at  $K = 2.4$ , the anomalies on 2, 4, and 5 days before EQs are significantly related to the EQs. Therefore, 5 days were taken as the lead time to EQs. Following this lead time, dates of such anomalies and corresponding EQs are listed in Table 1 and in the upper left area of Figure 1, respectively.

[12] Two kinds of rates may be defined on the relation between EQs and preseismic anomalies. One is EQ occur-

rence rate which is the number of preseismic anomalies divided by the total number of the anomalies. The other is the anomaly appearance rate which is the number of EQs with anomalies divided by the total number of EQs. Figure 4 shows curves depicting how the two rates depend on the threshold  $K$  and de-clustering of anomalies and EQs. In the present study,  $K = 2.4$ , which is the  $K$  value near the cross point of the curves, was chosen because the sum of the two rates is largest at this  $K$  value.

[13] Figure 5 shows the raw data of the received EM waves. In Figure 5c, the enhancement of the intensity in both polarizations is attributed to the plasma scattering in ionosphere [see *Smith and Matsushita, 1962; Ichinose and Kainuma, 1996*]. In the case of the meteor shower and Es-layer appearance, both polarizations were enhanced because the shapes of the reflecting or scattering planes have roughness. As the example of Figure 5d shows, only horizontal component is enhanced in the case of preseismic anomalies. This may indicate the possibility of the transmission through the atmosphere [see *Burrows, 1968*].

### 4. Conclusion

[14] According to the criteria employed in this work, the preseismic anomalies appeared within 5 days before the  $M \geq 4.8$  EQs were their precursors. The polarization

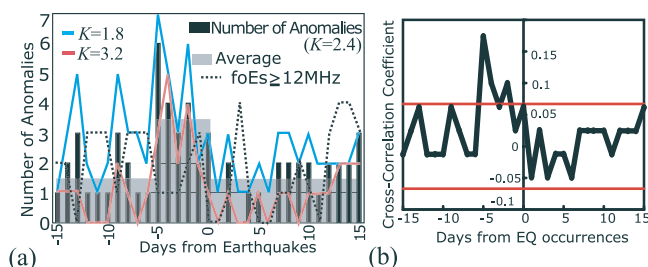


**Figure 3.** (a) The number of the anomalies within 15 days before and after the EQs. Aftershocks are excluded. Dotted line represents the number of Es-layer days ( $foEs \geq 12$  MHz) at Kokubunji. (b) Cross-correlation coefficient between EQs and anomalies with time lag. The approximate z-test at significance level 0.10 was applied [see *Bickel and Doksum, 2001*]. The null hypothesis (between red lines) is rejected at this significance level.

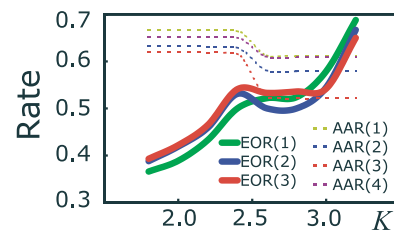


**Figure 4.**  $K$ -dependence of the EQ occurrence rate (EOR) and the anomaly appearance rate (AAR). For counting EQ and anomaly numbers, de-clustering was performed. AAR (1): EQs within 3 days were de-clustered. AAR (2): within 2 days. AAR (3): within 1 day. AAR (4): no de-clustering. AAR (3) that is least over-counting, if any, was adopted. Corresponding criteria for EOR were also introduced. Note that the criterion that corresponds to AAR (3) does not exist. EOR (1): Anomalies within 3 days. EOR (2): within 2 days. EOR (3): no de-clustering. EOR (1) and EOR (3) seem to have the least over-counting depending on  $K$ . EOR (3), closing to AAR (3), was selected. For de-clustering, the occurrence and the appearance date were assigned the first and the last date, respectively.

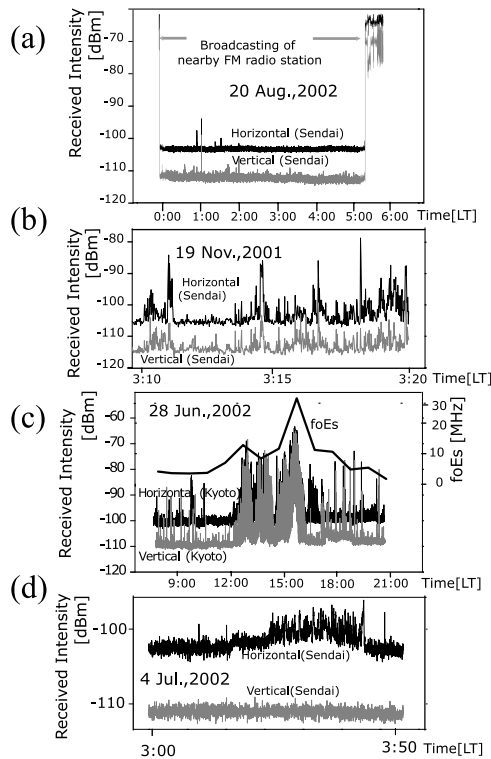


**Figure 5.** Raw data of the received VHF EM waves. (a) Normal day. (b) Leonids meteor shower. (c) Es-layer variations. (d) Preseismic anomaly.

of the received over-the-horizon EM waves was only horizontal, which indicated that the propagation path was not in the ionosphere, but in the atmosphere. The anomalies, therefore, may be better termed “atmospheric anomalies”.

[15] **Acknowledgments.** The authors would like to thank Prof. S. Uyeda (Tokai University) for the useful discussions. Co-first authors contributed equally to this work.

## References

- Bickel, P. J., and K. A. Doksum (2001), *Mathematical Statistics: Basic Ideas and Selected Topics*, 2nd ed., Prentice-Hall, Old Tappan, N. J.
- Burrows, V. G. (1968), *VHF Radio Propagation in the Troposphere*, Int. Textbooks, Scranton, Pa.
- Davies, K. (1990), *Ionospheric Radio*, Peter Peregrinus, London.
- Kushida, Y., and R. Kushida (2002), Possibility of earthquake forecast by radio observations in the VHF band, *J. Atmos. Electr.*, 22, 239–255.
- Ichinose, M., and S. Kainuma (1996), Polarization characteristics of VHF radio waves reflected by the Es-Layer, *IEEE Trans. Broadcasting*, 42, 82–87.
- Molchanov, O. A., and M. Hayakawa (1998), Subionospheric VLF signal perturbations possibly related to earthquakes, *J. Geophys. Res.*, 103, 17,489–17,504.
- Liu, J. Y., Y. I. Chen, S. A. Pulinet et al. (2000), Seismo-ionospheric signatures prior to  $M \geq 6.0$  Taiwan earthquakes, *Geophys. Res. Lett.*, 27, 3113–3116.
- Sakai, K., T. Takano, and S. Shimakura (2001), Observation system for anomalous propagation of FM radio broadcasting wave related to earthquakes and its preliminary result, *J. Atmos. Electr.*, 21, 71–78.
- Smith, E. K., Jr., and S. Matsushita (Eds.) (1962), *Ionospheric Sporadic E*, Pergamon, New York.

H. Fujiwara and Y. H. Ohtsuki, Department of Physics, Waseda University, Shinjuku-ku, Tokyo, 169-8555, Japan.

M. Kamogawa and H. Sakata, Department of Physics, Tokyo Gakugei University, 4-1-1, Nukuikitamachi, Koganei-shi, Tokyo, 184-8501, Japan. (kamogawa@u-gakugei.ac.jp)

M. Ikeda, Shintech Co. Ltd., Hachioji, Tokyo, 192-0044, Japan.

J. Y. Liu, Institute of Space Science, National Central University, Chung-Li, 32054, Taiwan.

Y. I. Chen, Institute of Statistics, National Central University, Chung-Li, 32054, Taiwan.

H. Ofurton, Tokyo Metropolitan College of Aeronautical Engineering, Arakawa-ku, Tokyo, 116-8523, Japan.

S. Muramatsu, San-Eye Co. Ltd., Imabari-shi, 794-0028, Japan.

Y. J. Chuo, Department of Information Management, Ling-Tung College, 408 Tai-Chung, Taiwan.